Analysis of Differentially Expressed Genes in Neuroendocrine Carcinomas of the Lung

Chigusa Okubo, MS, Yuko Minami, MD,*§ Ryota Tanaka, MD,*‖ Teruhito Uchihara, MD,*¶ Yoichi Anami, MD,* Shuichiroh Furuya, BA,‡ Yukio Morishita, MD,† Tatsuo Iijima, MD,* and Masayuki Noguchi, MD**

Introduction: Large cell neuroendocrine carcinoma (LCNEC) and small cell lung carcinoma (SCLC) show considerable differences in their histology but share neuroendocrine (NE) characteristics and also genetic and/or expression patterns.

Methods: We used the subtractive expression method to identify differences in gene expression that would allow discrimination between these two types of NE lung carcinoma.

Results: Eight cDNA fragments were transcribed at a higher level in LCNEC compared with SCLC, and these corresponded to five mitochondrial genes, two ribosomal genes, and one fetal regulation factor, neuronatin (NNAT). Immunohistochemically, NNAT protein was detected in 43% (6/14) of LCNECs but in only 8% (1/13) of SCLCs ($p < 0.05$). Positive staining for NNAT was observed in areas that did not show the NE morphology, such as palisading and rosettes.

Conclusions: The present results suggest that NNAT has the potential to be used as a differential maker between LCNEC and SCLC.

Key Words: Lung, Neuroendocrine carcinoma, Neuronatin, Suppression subtractive hybridization, TALPAT.

(*J Thorac Oncol.* 2006;1: 780–786)

Neuroendocrine (NE) lung tumors include four histological types: typical carcinoid tumor, atypical carcinoid tumor, large cell neuroendocrine carcinoma (LCNEC), and small cell lung carcinoma (SCLC).[1] NE tumors are usually distinguished from non-NE tumors by several histological characteristics, such as organoid nesting, palisading, rosettes, or trabeculae. Immunohistochemically, they are positive for antibodies to NE markers, such as antichromogranin A (CGA), antisynaptophysin (SYN), and anti-CD56 antibodies. Among the four histological subtypes, carcinoid tumors have distinctive histological characteristics and show extremely favorable prognoses. On the other hand, the latter two tumors are highly malignant, and no difference was noted between the two.[2,3] There are histological and morphological criteria that can be used to distinguish between LCNEC and SCLC, but the histological border between them is unclear.

LCNEC and SCLC have many similarities in their genetic characteristics. Recently, many studies have focused on discrimination between LCNEC and SCLC. Comparative genomic hybridization has revealed that several chromosomal aberrations, namely, loss of 3p, 4q, 5q and 13q, and gain of 5p, appear in both of them, but gain of 3q is only observed in SCLC.[4,5] Shin et al.[6] screened for loss of heterozygosity (LOH) and examined the location of putative tumor suppressor genes on 5q using 19 microsatelite makers covering 13 primary LCNECs. However, they did not examine or compare these results with other histological tumors. Kobayashi et al.[7] analyzed LOH of candidate loci that had previously been reported to be associated with human lung cancers: CI31107 (3p), D3S1300 (3p), D5S644 (5q), D9S171 (9p), mdf220 (9q), D11S4938 (11q), RBi2 (13q), and TP53 (17p).[8–15] They confirmed that frequencies of alteration were greater than 50%, except for D9S171, with LCNEC and SCLC showing similar allelic loss patterns. Hiroshima et al.[16] reported LOH and methylation status of LCNEC, SCLC, and classic large cell carcinoma. They concluded that genetic alteration of LCNEC was akin to those of SCLC; however, allelic losse at 5q and abnormalities in the p16 gene may differentiate LCNEC from SCLC. Zaffaroni et al. used the telomeric repeat amplification protocol assay to show that telomeric signals of LCNEC and SCLC were of equally high frequency (93 and 87%).[17] Expression profiling with cDNA microarrays led to the proposal that LCNEC and SCLC should be reclassified as a single group of high-grade NE tumors,[18–20] but no samples of each gene showing distinctive expression pattern were further analyzed. Protein expression has also been analyzed by a number of approaches using immunohistochemistry (IHC), and attempts to classify these tumors by IHC methods have used marker proteins such as

*Department of Pathology, Institute of Basic Medical Sciences, Graduate School of Comprehensive Human Sciences, and †Department of Clinical Pathology, Institute of Clinical Medicine, Graduate School of Comprehensive Human Sciences, University of Tsukuba, Ibaraki, Japan; ‡Department of Pathology, University Hospital of Tsukuba, Ibaraki, Japan; §Medical Oncology, Dana-Farber Cancer Institute, Boston, MA; ‖Department of Thoracic Surgery, Gunma Prefectural Cancer Center, Gunma, Japan; and ¶Department of Internal Medicine, Division of Infectious Diseases, Graduate School and Faculty of Medicine, University of the Ryukyus, Okinawa, Japan.

Address for correspondence: Masayuki Noguchi, MD, Department of Pathology, Institute of Basic Medical Sciences, University of Tsukuba 1-1-1 Tennodai, Tsukuba-shi, Ibaraki 305-8575, Japan. E-mail: nmasayuk@md.tsukuba.ac.jp

ISSN: 1556-0864/06/0108-0780

thyroid transcription factor 1, c-kit, fascin, TP53, retinoblastoma gene, and Bcl2–Bax expression balance. However, none of these methods were able to demonstrate marked differences between the two NE tumors.[7,21–27] Conspicuously, p16 was observed more frequently in SCLC (93%) than in LCNEC (58%).[16]

In the present study, we compared the mRNA expression profiles of LCNEC and SCLC by using suppression subtractive hybridization (SSH), which is a very powerful method for examining differences between expressed mRNAs,[28,29] with the intention of identifying unique genetic markers for discrimination between LCNEC and SCLC.

MATERIALS AND METHODS

Clinical Samples and Cell Line

Formalin-fixed, paraffin-embedded surgical tissue samples of 14 cases of LCNEC and 13 cases of SCLC were obtained from the pathology files of the University Hospital of Tsukuba (Ibaraki, Japan) from 1981 to 2006 and of Ibarakihigashi National Hospital (Ibaraki, Japan) from 1997 to 2005. The pathological and the clinical staging are shown in Table 1. The histological diagnoses of all specimens examined were reviewed by Y. Minami, T. Iijima, Y. Morishita, and M. Noguchi according to the histological typing criteria of lung tumors (World Health Organization, 3rd ed., 1999)[1] and the criteria of Travis et al.[30] In total, 27 cases of LCNEC and SCLC were subjected to IHC analysis.

Among the 14 LCNECs, fresh frozen material was available from case 8 (Figure 1a) and was used for the subtractive analysis. For SCLC, we used the human SCLC cell line Lu139, donated by the National Cancer Center Research Institute (Tokyo, Japan).

Five-week-old female SCID mice with a CB-17 genetic background were obtained from CLEA Japan, Inc. (Tokyo,

TABLE 1. Immunohistochemistry (IHC) for neuronatin and neuroendrocrine markers

		pTNM					IHC for Neuroendocrine Markers			
Case No.	Gender	T	N	M	pStage	Disease Stage	CGA	SYN	CD56	IHC NNAT
LCNEC										
1	M	2	0	0	IB		—	—	+	—
2	M	2	0	0	IB		—	—	+	—
3	M	1	0	0	IA		+	+	+	+
4	M	2	1	0	IIB		+	+	—	—
5	M	3	1	0	IIIA		+	+	—	—
6	M	4	2	0	IIIB		—	—	+	—
7	M	2	0	0	IB		—	—	+	+
8	M	2	0	0	IB		+	+	+	+
9	M	2	*	0	≥I		+	+	+	—
10	M	2	0	0	IB		+	+	+	+
11	M	1	*	0	≥I		—	+	+	+
12	M	2	1	0	IIB		+	—	+	+
13	M	1	0	0	IA		+	+	—	—
14	F	1	0	0	IA		+	—	+	—
SCLC										
15	M	1	2	0	IIIA	LD	—	—	—	—
16	M	1	0	1	IV	ED	+	+	+	+
17	M	2	1	0	IIB	LD	+	+	+	—
18	M	2	0	0	IB	LD	—	+	+	—
19	M	1	0	0	IA	LD	+	+	+	—
20	M	1	1	0	IIA	LD	+	+	+	—
21	M	2	2	0	IIIA	LD	—	+	+	—
22	F	1	1	0	IIA	LD	+	+	+	—
23	M	1	0	0	IA	LD	+	+	+	—
24	M	1	*	0	≥I	LD	—	—	+	—
25	M	1	0	0	IA	LD	+	+	+	—
26	M	2	1	0	IIB	LD	+	+	+	—
27	M	1	0	0	IA	LD	—	—	+	—
Mouse tumor with Lu139							—	+	+	—

Small cell lung carcinoma (SCLC) confined to the primary site, with or without regional lymph node involvement, was classified as limited disease (LD), whereas spread of disease beyond locoregional boundaries was considered extensive disease (ED). CGA, chromogranin A; SYN, synaptophysin; NNAT, neuronatin; LCNEC, large cell neuroendocrine carcinoma. *Lymph node dissection was not performed.

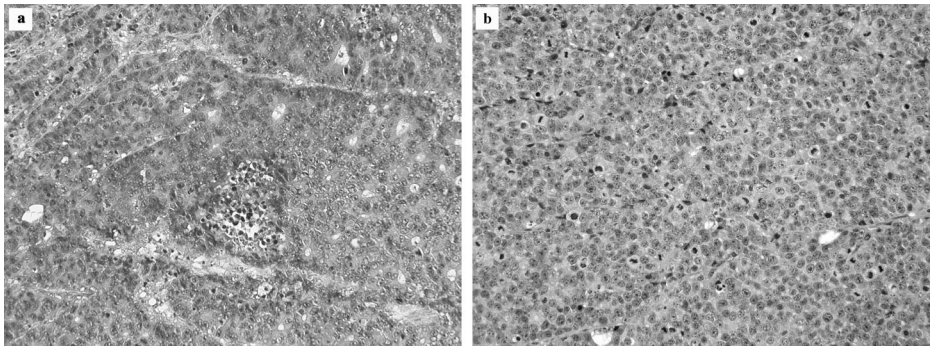

FIGURE 1. Histological appearance of a case of LCNEC (case 8, *a*) and a mouse Lu139 tumor (*b*). The LCNEC showed neuroendocrine morphology (e.g., organoid nesting, palisading, and trabeculae). The mouse tumor showed diffuse growth of small tumor cells with a high N/C ratio, mimicking human SCLC. (H.E.; original magnification, ×200.)

Japan). The mice were free of known pathogens at the time of the study and were housed in sterilized filter-topped cages and fed autoclaved food and water ad libitum. Cultured Lu139 cells, prepared at 1.0×10^7 cells/ml with medium, were inoculated subcutaneously into 10 SCID mice.

All mice were sacrificed after 2 months, and the subcutaneous tumors that had developed were fixed in 10% buffered formalin and embedded in paraffin. The paraffin sections were stained with hematoxylin and eosin. The diagnosis of SCLC was confirmed both histologically and using IHC (Figure 1b).

mRNA Amplification by T7 RNA Polymerase Promoter-Attached, Adaptor Ligation-Mediated, and PCR Amplification followed by in vitro T7-Transcription (TALPAT)

Separate mRNA samples extracted from fresh frozen tissue of a case of LCNEC and from cultured Lu139 cells, which are a model for SCLC, were amplified by the TALPAT method.[31] This procedure enables very small amounts of mRNA to be amplified with faithful maintenance of the relative levels of mRNA expression. Briefly, TALPAT consists of five enzymatic reaction steps forming a modification to the SuperScript™ Choice system (Invitrogen Corp., Carlsbad, CA): step 1, cDNA synthesis with an oligo(dT)-T7 promoter primer (5′-pGGCCAGTGAATTGTAATACGACTCACTATAGGGAGGCGGTTTTTTTTTTTTTTTTTTTT-TTT-3′); step 2, cRNA amplification by in vitro transcription using T7 RNA polymerase (Ambion Inc., Austin, TX); step 3, cDNA synthesis with $pd(N)_6$ random hexamer (Amersham Biosciences Corp., Piscataway, NJ) for first-strand cDNA and oligo(dT)-T7 promoter primer for second-strand cDNA; step 4, adaptor ligation-mediated PCR; and step 5, cRNA amplification by in vitro transcription using T7 RNA polymerase.

SSH

SSH between the TALPAT samples from LCNEC tissue and SCLC cell line was performed with a Superscript™ Choice System (Invitrogen Corp.) and a PCR-Select™ cDNA Subtraction Kit (BD Bioscience Clontech, Palo Alto, CA) with modifications. In brief, after preparation of the double-stranded cDNAs from each TALPAT sample, the cDNA was digested with *Rsa* I and ligated to adaptors supplied with the PCR-Select™ cDNA Subtraction Kit. Two-directional (forward and reverse) subtractive hybridizations and unsubtractive hybridizations were performed between LCNEC tissue and SCLC cell line, and the subtractive hybridization products were amplified by suppression PCR according to the manufacturer's instructions.

Semiquantitative Screening of the Subtracted cDNA Libraries

The overexpressed cDNA pool from the LCNEC tissue (forward subtracted cDNA) was cloned into the PCR 2.1 vector (Invitrogen Corp.). One hundred seventy-six bacterial colonies were randomly picked up, and their inserted cDNAs were amplified by PCR. The PCR products, together with amplified beta-actin fragments as internal controls, were blotted onto nylon membranes. ^{32}P-labeled probes were made from LCNEC and SCLC cell cDNAs from TALPAT step 4 and were hybridized separately. Subsequently, the intensity of each ^{32}P signal was represented numerically, and the expression score of each clone was normalized with that of beta-actin. The average score for all clones of each gene was calculated, and clones that were up-regulated in LCNEC compared with SCLC were identified.

Sequence Analysis

The clones of genes highly expressed in LCNEC were sequenced with a BigDye Terminator v3.1 Cycle Sequencing Ready Reaction Kit and an ABI PRISM 310 Genetic Analyzer (both from Applied Biosystems Japan Ltd., Tokyo, Japan).

IHC

For IHC, 14 cases of LCNEC, 13 cases of SCLC, and the SCID mouse Lu139 tumor were analyzed. Prepared 3-μm-thick paraffin sections were deparaffinized and autoclaved in citrate buffer (pH 6.0) for 15 minutes for retrieval of their antigenicity. Inhibition of endogenous peroxidase activity was performed for 5 minutes with DAKO ChemMate peroxidase blocking solution (DakoCytomation, Glostrup, Denmark). The polyclonal antibodies against CGA and SYN (DakoCytomation) and monoclonal antibody against CD56 (Nippon Kayaku, Tokyo, Japan) were used for immunohistochemical NE markers. The polyclonal antibody against neuronatin (NNAT) (Santa Cruz Biotechnology, Inc., Santa Cruz, CA) was diluted 1:200 and incubated at room temperature for 30 minutes. Subsequently, the specimens were treated with the link antibody (biotinylated antigoat immunoglobulin) and

TABLE 2. Summary of cDNA clones that were highly expressed in large cell neuroendocrine carcinoma

Description	Number of Clones	mRNA expression score†		
		LCNEC	SCLC	LCNEC/SCLC
NADH dehydrogenase 1	6	1.133	0.300	3.78
NADH dehydrogenase 3	3	0.967	0.467	2.07
Cytochrome c oxidase III	4	0.725	0.150	4.83
Cytochrome b	16	0.638	0.100	6.38
ATP synthase 6	26	0.892	0.246	3.63
Ribosomal protein L31	1	1.100	0.600	1.83
Ribosomal protein S24	10	0.790	0.130	6.08
Neuronatin	1	1.400	0.800	1.75

†Each mRNA expression score was normalized with beta-actin (1.0), and the average of the mean scores of all clones was calculated.

then with streptavidin conjugated to horseradish peroxidase (LSAB+ kit; DakoCytomation) for 15 minutes according to the manufacturer's instructions. Finally, staining was visualized by exposure to 3,3′-diaminobenzidine for 5 minutes, and the slides were counterstained with hematoxylin. Negative controls were prepared by omitting the primary antibody. We judged the result as positive when more than 5% of tumor cells were stained by the antibody, and then the statistical difference was determined by Fisher's extract test. Differences were considered significant when $p < 0.05$.

RESULTS

Total RNAs were extracted from frozen tissue blocks of LCNEC (case 8, Figure 1a) and from cultured Lu139 cells. Then, 100 ng of each total RNA were amplified by the TALPAT method, resulting in over 10 mg of cRNAs. After SSH analysis, 176 clones were chosen randomly from the library of cDNAs overexpressed in LCNEC compared with SCLC and blotted onto nylon membranes. Differential expression of these clones was confirmed using probes prepared from the cDNA products of TALPAT step 4 (see Materials and Methods). As Table 2 shows, 67 up-regulated cDNA clones in LCNEC were selected after semiquantitative screening followed by sequencing. Some clones contained cDNA fragments of the same gene, and we finally identified eight genes that showed differential expression between LCNEC (case 8) and SCLC (Lu139).

High expression of mRNAs for the selected genes was confirmed by in situ hybridization (ISH) with formalin-fixed, paraffin-embedded tissue samples of case 8 and mouse Lu139 tumor (data not shown). Among the genes detected in this study, most were coded for components of mitochondria or ribosomes that can be considered housekeeping proteins. Therefore, we selected NNAT, which is related to neuronal development in the fetal stage and neonatal period, for further examination of whether it could distinguish between LCNEC and SCLC.

To confirm the expression of NNAT at the protein level, we examined surgically resected, formalin-fixed, paraffin-embedded LCNEC and SCLC cases by IHC using a polyclonal antibody against NNAT. The results of IHC staining for NNAT and for three general NE markers are summarized in Table 1. Six of 14 LCNECs (42.9%) and 1 of 13 SCLCs (7.7%) showed a positive reaction against the anti-NNAT antibody in the cytoplasm of carcinoma cells (Figure 2). However, no normal tissues or cells showed positive reaction against the antibody. LCNEC showed significantly high frequency of NNAT than SCLC ($p = 0.048$). Interest-

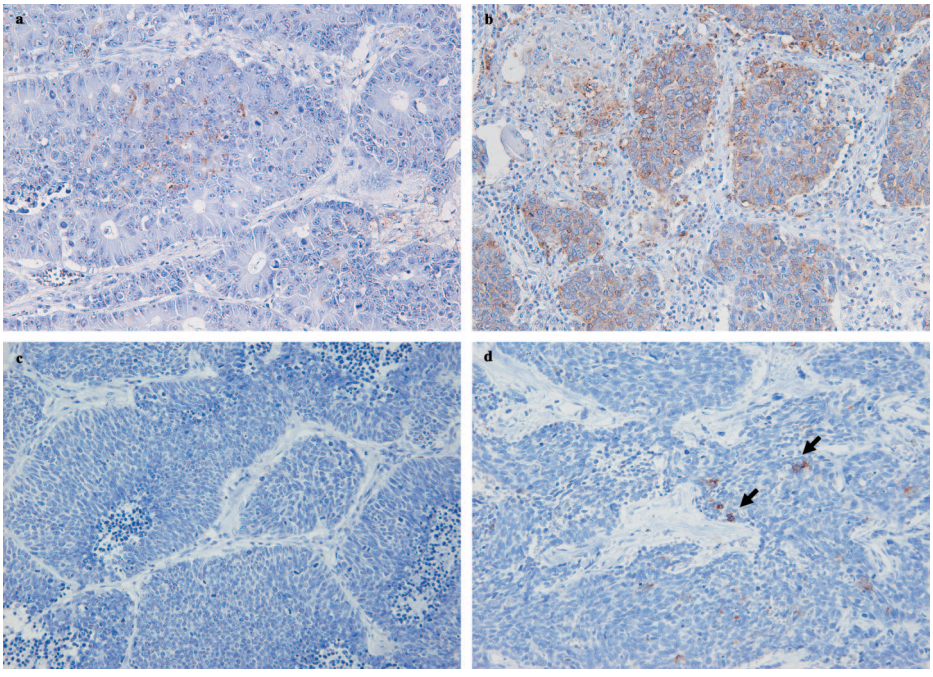

FIGURE 2. Immunohistochemical staining for NNAT in LCNEC and SCLC. Areas showing NE morphology, such as palisading or rosette formation, were negative for the antibody (case 8, *a*), but poorly differentiated areas showed positive reaction (case 3, *b*). All cases of SCLC were negative (e.g., case 20, *c*) except for case 16 (d), which contained partially positive cells (*arrows*). (Original magnification, ×200.)

ingly, areas with NE morphology did not show positive reaction for anti-NNAT antibody (Figure 2a).

As for the three general NE markers—CGA, SYN and CD56—10 LCNECs expressed multiple general NE markers; four cases stained for all three markers, and six cases stained for two markers. The other four cases showed positive staining for one of the three NE markers. Eight of the SCLCs were reactive for all three markers, two cases were reactive for two markers, and two cases were reactive for one marker. The other case showed negative reaction for all three NE markers. Intriguingly, the LCNEC cases that were positive for anti-NNAT antibody showed positive reaction against 2.33 general NE markers on average, but the negative cases showed positive reaction against only 1.75 NE markers. In SCLCs, there were several cases that did not show positive reaction against all the general NE markers, but the NNAT positive case (case 13) was positive against all three NE markers. In any case, the differences in NNAT expression against expression of general NE markers in LCNEC and SCLC were also not significant.

DISCUSSION

In this study, we analyzed the differences between LCNEC and SCLC at the transcriptional level. A frozen sample of LCNEC that showed representative NE morphology and reactivities for NE markers without any therapy before surgery was used for mRNA extraction (Figure 1a). For SCLC, on the other hand, we used a SCLC cell line because some cases of SCLC had been treated with anticancer drugs before surgery and because frozen tissue was not available for the other cases. The Lu139 SCLC cell line, which is positive for SYN and CD56 but negative for CGA, was chosen. The tumors that developed in mice after inoculation of Lu139 maintained the histological characteristics of human SCLC and the NE phenotype (Figure 1b).

Many studies have tried to find phenotypic or genetic differences between LCNEC and SCLC, but few have succeeded in defining different characteristics. Transcriptome analysis has also been performed by the cDNA microarray method, leading Virtanen et al.[19] to suggest that the two disease entities should be considered as a single type of NE cancer with high malignancy. In this study, we also examined cDNA expression profiles but used another powerful technique for cDNA analysis, namely, a combination of the TALPAT[31] and SSH[29] methods. TALPAT enable us to get huge amount of cDNA from a little sample, and SSH, a cloning method, can construct cDNA libraries that are distinctively expressed in one sample compared with the other sample.[32–35] cDNA microarray methods, in contrast, are useful for clustering gene expression patterns for many cases, but these methods do not focus on calculating alterations of individual gene expression levels or on cloning particular genes.[18–20] We were able to identify eight cDNA clones that showed higher transcription in LCNEC than in SCLC.

The eight cDNA fragments included five mitochondrial genes, two ribosomal genes, and a regulation factor for ion channels, NNAT (Table 2). The transcribed products of NADH dehydrogenase 1 and 3 are components of complex I (NADH:ubiquinone oxidoreductase), which is located within the mitochondrial inner membrane and is the first step in the electron transport chain of mitochondrial oxidative phosphorylation. Cytochrome c oxidase III is one of the three subunits of respiratory complex IV, which is the third and final enzyme of the electron transport chain of mitochondrial oxidative phosphorylation. Mutation of the cytochrome b gene leads to phenotypically relevant alleles that contribute to disorders such as Laber hereditary optic neuropathy,[36–38] colorectal cancer,[39,40] and obesity.[41] Torigoe et al. reported that ATP synthase 6 is up-regulated in response to antineoplastic agents such as an antiapoptotic defense.[42] In mammalian ribosomes, the organelles that catalyze protein synthesis, the ribosomal protein S24 and L31 genes, encode proteins that are components of the small 40S subunit and the large 60S subunit, respectively. These seven genes are thought to be highly conserved and act as so-called housekeeping genes. On the other hand, the protein encoded by the NNAT gene is a proteolipid that may be involved in the regulation of ion channels during brain development.[43,44] In general, NNAT is expressed in the mammalian fetus but not in adults,[45] suggesting a specific role for NNAT expression in tumor tissue and causing us to focus on the characteristics of this aberrant expression. To confirm the localization of expression of NNAT, we used ISH to show that mRNA expression occurred in carcinoma cells and also transplanted tumor cells in mice.

NNAT maps to human chromosome 20q11.2-q12[43,44] and mouse distal chromosome 2[46] and is one of the imprinted genes[47–49] whose regulation may involve noncoding RNAs[49–51] and/or methylation of CpG islands.[47,52] The amino acid sequence of NNAT is homologous to that of the proteolipids peroxisomal membrane protein-1 and phospholamban,[44] and it therefore constitutes a putative member of the proteolipid family. Expression of mRNA for NNAT occurs in the central nervous system from midgestation through early postnatal development,[44,45,53] correlating with the onset and termination of brain development in mice and humans. High expression levels of NNAT have been reported in certain pathological settings such as prostate tumors,[54] medulloblastomas,[32] pituitary adenomas,[55] and tamoxifen-resistant breast cancer.[56]

We used IHC to analyze the protein expression of NNAT in LCNEC and SCLC. As shown in Table 1, 6 of 14 cases of LCNEC (42.9%) and 1 of 13 cases of SCLC (7.7%) were positive for NNAT. Cases of LCNEC express NNAT protein more frequently than cases of SCLC did, and the difference between these frequencies was statistically significant ($p = 0.048$, Fisher's extract test). The staining for NNAT in LCNECs appeared heterogeneous. Interestingly, NNAT protein was negative in areas that showed NE morphology, such as peripheral palisadings and rosettes (Figure 2a, b). In SCLCs, we could demonstrate positivity for NNAT in only one case, and the positive cells were localized in small foci (Figure 2c, d). On the other hand, the LCNECs expressing NNAT showed positive reaction for more general NE markers than LCNECs that were negative for NNAT (2.33 versus 1.75). Furthermore, the positive SCLC for anti-NNAT antibody (case 13) showed positive reaction for all three NE

markers. Correlation between NNAT expression and expression of NE markers in LCNEC and also in SCLC was not statistically significant. Additionally, NNAT was not detected in nontumorous lung tissue or in any other normal organs. Putting together the results of IHC of NNAT and general NE markers, we speculated that NNAT has the potential to act as a tumor marker for IHC and/or serodiagnosis.

We examined only a very limited number of cases in this study, and we were unable to demonstrate a relationship between the expression of NNAT and prognosis. A larger case series, including not only NE carcinomas but also carcinoid tumors and non-NE carcinomas, should be examined for the expression of NNAT to elucidate the clinicopathological significance of expression of this gene.

REFERENCES

1. Travis WD, Colby TV, Corrin B, et al. *World Health Organization. International Histological Classification of Tumors. Histological Typing of Lung and Pleural Tumors*, 3rd ed. Berlin: Springer, 1999.
2. Travis WD, Rush W, Flieder DB, et al. Survival analysis of 200 pulmonary neuroendocrine tumors with clarification of criteria for atypical carcinoid and its separation from typical carcinoid. *Am J Surg Pathol* 1998;22:934–944.
3. Asamura H, Kameya T, Matsuno Y, et al. Neuroendocrine neoplasms of the lung: a prognostic spectrum. *J Clin Oncol* 2006;24:70–76.
4. Ullmann R, Schwendel A, Klemen H, et al. Unbalanced chromosomal aberrations in neuroendocrine lung tumors as detected by comparative genomic hybridization. *Hum Pathol* 1998;29:1145–1149.
5. Ullmann R, Petzmann S, Sharma A, et al. Chromosomal aberrations in a series of large-cell neuroendocrine carcinomas: unexpected divergence from small-cell carcinoma of the lung. *Hum Pathol* 2001;32:1059–1063.
6. Shin JH, Kang SM, Kim YS, et al. Identification of tumor suppressor loci on the long arm of chromosome 5 in pulmonary large cell neuroendocrine carcinoma. *Chest* 2006;128:2999–3003.
7. Kobayashi Y, Tokuchi Y, Hashimoto T, et al. Molecular markers for reinforcement of histological subclassification of neuroendocrine lung tumors. *Cancer Sci* 2004;95:334–341.
8. Jones MH, Yamakawa K, Nakamura Y. Isolation and characterization of 19 dinucleotide repeat polymorphisms on chromosome 3p. *Hum Mol Genet* 1992;1:131–133.
9. Tokuchi Y, Kobayashi Y, Hayashi S, et al. Abnormal FHIT transcripts found in both lung cancer and normal lung tissue. *Genes Chromosomes Cancer* 1999;24:105–111.
10. Wieland I, Bohm M, Arden KC, et al. Allelic deletion mapping on chromosome 5 in human carcinomas. *Oncogene* 1996;12:97–102.
11. Gyapay G, Morissette J, Vignal A, et al. The 1993-94 Genethon human genetic linkage map. *Nat Genet* 1994;7:246–339.
12. Kwiatkowski DJ, Henske EP, Weimer K, et al. Construction of a GT polymorphism map of human 9q. *Genomics* 1992;12:229–240.
13. Manickam P, Guru SC, Debelenko LV, et al. Eighteen new polymorphic markers in the multiple endocrine neoplasia type 1 (MEN1) region. *Hum Genet* 1997;101:102–108.
14. Toguchida J, McGee TL, Paterson JC, et al. Complete genomic sequence of the human retinoblastoma susceptibility gene. *Genomics* 1993;17:535–543.
15. Jones MH, Nakamura Y. Detection of loss of heterozygosity at the human TP53 locus using a dinucleotide repeat polymorphism. *Genes Chromosomes Cancer* 1992;5:89–90.
16. Hiroshima K, Iyoda A, Shibuya K, et al. Genetic alterations in early-stage pulmonary large cell neuroendocrine carcinoma. *Cancer* 2004;100:1190–1198.
17. Zaffaroni N, De Polo D, Villa R, et al. Differential expression of telomerase activity in neuroendocrine lung tumours: correlation with gene product immunophenotyping. *J Pathol* 2003;201:127–133.
18. Bhattacharjee A, Richards WG, Staunton J, et al. Classification of human lung carcinomas by mRNA expression profiling reveals distinct adenocarcinoma subclasses. *Proc Natl Acad Sci USA* 2001;98:13790–13795.
19. Virtanen C, Ishikawa Y, Honjoh D, et al. Integrated classification of lung tumors and cell lines by expression profiling. *Proc Natl Acad Sci USA* 2002;99:12357–12362.
20. Jones MH, Virtanen C, Honjoh D, et al. Two prognostically significant subtypes of high-grade lung neuroendocrine tumours independent of small-cell and large-cell neuroendocrine carcinomas identified by gene expression profiles. *Lancet* 2004;363:775–781.
21. Sturm N, Lantuejoul S, Laverriere MH, et al. Thyroid transcription factor 1 and cytokeratins 1, 5, 10, 14 (34betaE12) expression in basaloid and large-cell neuroendocrine carcinomas of the lung. *Hum Pathol* 2001;32:918–925.
22. Sturm N, Rossi G, Lantuejoul S, et al. Expression of thyroid transcription factor-1 in the spectrum of neuroendocrine cell lung proliferations with special interest in carcinoids. *Hum Pathol* 2002;33:175–182.
23. Araki K, Ishii G, Yokose T, et al. Frequent overexpression of the c-kit protein in large cell neuroendocrine carcinoma of the lung. *Lung Cancer* 2003;40:173–180.
24. Pelosi G, Pasini F, Fraggetta F, et al. Independent value of fascin immunoreactivity for predicting lymph node metastases in typical and atypical pulmonary carcinoids. *Lung Cancer* 2003;42:203–213.
25. Brambilla E, Negoescu A, Gazzeri S, et al. Apoptosis-related factors p53, Bcl2, and Bax in neuroendocrine lung tumors. *Am J Pathol* 1996;149:1941–1952.
26. Jiang SX, Kameya T, Shinada J, et al. The significance of frequent and independent p53 and bcl-2 expression in large-cell neuroendocrine carcinomas of the lung. *Mod Pathol* 1999;12:362–369.
27. Gouyer V, Gazzeri S, Bolon I, et al. Mechanism of retinoblastoma gene inactivation in the spectrum of neuroendocrine lung tumors. *Am J Respir Cell Mol Biol* 1998;18:188–196.
28. Gurskaya NG, Diatchenko L, Chenchik A, et al. Equalizing cDNA subtraction based on selective suppression of polymerase chain reaction: cloning of Jurkat cell transcripts induced by phytohemaglutinin and phorbol 12-myristate 13-acetate. *Anal Biochem* 1996;240:90–97.
29. Diatchenko L, Lau YF, Campbell AP, et al. Suppression subtractive hybridization: a method for generating differentially regulated or tissue-specific cDNA probes and libraries. *Proc Natl Acad Sci USA* 1996;93:6025–6030.
30. Travis WD, Linnoila RI, Tsokos MG, et al. Neuroendocrine tumors of the lung with proposed criteria for large-cell neuroendocrine carcinoma. An ultrastructural, immunohistochemical, and flow cytometric study of 35 cases. *Am J Surg Pathol* 1991;15:529–553.
31. Aoyagi K, Tatsuta T, Nishigaki M, et al. A faithful method for PCR-mediated global mRNA amplification and its integration into microarray analysis on laser-captured cells. *Biochem Biophys Res Commun* 2003;300:915–920.
32. Yokota N, Mainprize TG, Taylor MD, et al. Identification of differentially expressed and developmentally regulated genes in medulloblastoma using suppression subtraction hybridization. *Oncogene* 2004;23:3444–3453.
33. Chen X, Halberg RB, Ehrhardt WM, et al. Clusterin as a biomarker in murine and human intestinal neoplasia. *Proc Natl Acad Sci USA* 2003;100:9530–9535.
34. Lee KF, Kwok KL, Chung MK, et al. Phospholipid transfer protein (PLTP) mRNA expression is stimulated by developing embryos in the oviduct. *J Cell Biochem* 2006;95:740–749.
35. Shackel NA, McGuinness PH, Abbott CA, et al. Novel differential gene expression in human cirrhosis detected by suppression subtractive hybridization. *Hepatology* 2003;38:577–588.
36. Brown MD, Voljavec AS, Lott MT, et al. Mitochondrial DNA complex I and III mutations associated with Leber's hereditary optic neuropathy. *Genetics* 1992;130:163–173.
37. Johns DR, Neufeld MJ. Cytochrome b mutations in Leber hereditary optic neuropathy. *Biochem Biophys Res Commun* 1991;181:1358–1364.
38. Mackey DA, Oostra RJ, Rosenberg T, et al. Primary pathogenic mtDNA mutations in multigeneration pedigrees with Leber hereditary optic neuropathy. *Am J Hum Genet* 1996;59:481–485.
39. Warburg O. On the origin of cancer cells. *Science* 1956;123:309–314.
40. Polyak K, Li Y, Zhu H, et al. Somatic mutations of the mitochondrial genome in human colorectal tumours. *Nat Genet* 1998;20:291–293.
41. Okura T, Koda M, Ando F, et al. Association of the mitochondrial DNA 15497G/A polymorphism with obesity in a middle-aged and elderly Japanese population. *Hum Genet* 2003;113:432–436.

42. Torigoe T, Izumi H, Ishiguchi H, et al. Enhanced expression of the human vacuolar H+-ATPase c subunit gene (ATP6L) in response to anticancer agents. *J Biol Chem* 2002;277:36534–36543.
43. Dou D, Joseph R. Structure and organization of the human neuronatin gene. *Genomics* 1996;33:292–297.
44. Dou D, Joseph R. Cloning of human neuronatin gene and its localization to chromosome-20q 11.2-12: the deduced protein is a novel "proteo-lipid." *Brain Res* 1996;723:8–22.
45. Kikyo N, Williamson CM, John RM, et al. Genetic and functional analysis of neuronatin in mice with maternal or paternal duplication of distal Chr 2. *Dev Biol* 1997;190:66–77.
46. Wijnholds J, Chowdhury K, Wehr R, et al. Segment-specific expression of the neuronatin gene during early hindbrain development. *Dev Biol* 1995;171:73–84.
47. Evans HK, Wylie AA, Murphy SK, et al. The neuronatin gene resides in a "micro-imprinted" domain on human chromosome 20q11.2. *Genomics* 2001;77:99–104.
48. Kagitani F, Kuroiwa Y, Wakana S, et al. Peg5/neuronatin is an imprinted gene located on sub-distal chromosome 2 in the mouse. *Nucleic Acids Res* 1997;25:3428–3432.
49. Kiyosawa H, Yamanaka I, Osato N, et al. Antisense transcripts with FANTOM2 clone set and their implications for gene regulation. *Genome Res* 2003;13:1324–1334.
50. Okazaki Y, Furuno M, Kasukawa T, et al. Analysis of the mouse transcriptome based on functional annotation of 60,770 full-length cDNAs. *Nature* 2002;420:563–573.
51. Kiyosawa H, Kawashima T, Silva D, et al. Systematic genome-wide approach to positional candidate cloning for identification of novel human disease genes. *Intern Med J* 2004;34:79–90.
52. Kuerbitz SJ, Pahys J, Wilson A, et al. Hypermethylation of the imprinted NNAT locus occurs frequently in pediatric acute leukemia. *Carcinogenesis* 2002;23:559–564.
53. John RM, Aparicio SA, Ainscough JF, et al. Imprinted expression of neuronatin from modified BAC transgenes reveals regulation by distinct and distant enhancers. *Dev Biol* 2001;236:387–399.
54. Hu Y, Ippolito JE, Garabedian EM, et al. Molecular characterization of a metastatic neuroendocrine cell cancer arising in the prostates of transgenic mice. *J Biol Chem* 2002;277:44462–44474.
55. Usui H, Morii K, Tanaka R, et al. cDNA cloning and mRNA expression analysis of the human neuronatin. High level expression in human pituitary gland and pituitary adenomas. *J Mol Neurosci* 1997;9:55–60.
56. Becker M, Sommer A, Kratzschmar JR, et al. Distinct gene expression patterns in a tamoxifen-sensitive human mammary carcinoma xenograft and its tamoxifen-resistant subline MaCa 3366/TAM. *Mol Cancer Ther* 2006;4:151–168.